

Exploring the relationship between particulate matter, CO, SO₂, NO₂, O₃ and urban heat island in Seoul, Korea

Jack Ngarambe, Soo Jeong Joen, Choong-Hee Han, Geun Young Yun *

Department of Architectural Engineering, Kyung Hee University, 1732, Deogyeong-daero, Giheung-gu, Yongin-si, Gyeonggi-do 17104, South Korea



ARTICLE INFO

Editor: L. Eder

Keywords:

Urban heat island
Air pollution
Mixing layer height
Mitigation strategies
Statistical analysis

ABSTRACT

Urban environments face two challenging problems that are parallel in nature but yet with compelling potential synergistic interactions; urban heat island (UHI) and air pollution. We explore these interactions using in-situ temperature and air pollution data collected from 13 monitoring stations for nine years. Through regression analysis and analysis of variance (ANOVA) tests, we found that carbon monoxide (CO), nitrogen dioxide (NO₂), sulfur dioxide (SO₂), and particulate matter (PM) show positive correlations with UHI intensity (UHII). At the same time, Ozone (O₃) was negatively correlated with UHII. Moreover, there was a substantial seasonal effect on the strength of the correlations between UHI and air pollution, with some air pollutants showing strong associations with UHI during certain seasons (i.e., winter and autumn). The strongest interactions were observed for NO₂ ($R^2 = 0.176$) and PM10 ($R^2 = 0.596$) during the wintertime and for SO₂ ($R^2 = 0.849$), CO ($R^2 = 0.346$), PM2.5 ($R^2 = 0.695$) and O₃ ($R^2 = 0.512$) during autumn. Understanding such interactions is essential for urban climate studies and our study provides a basis for scientific discussions on integrative mitigation strategies for both UHI and air pollution in Seoul city.

1. Introduction

Urban areas experience drastic land-use changes as a result of increased urbanization. A by-product of such rapid land-use changes is a climate altered from its natural state in urban areas compared to the surrounding rural and suburban areas (Cui and Shi, 2012). For example, due to the altered natural state of land surfaces in urban areas which result in reduced albedo, increased solar storage capacities and distorted energy balances in urban atmospheres, urban areas tend to be relatively warmer than their rural and suburban counterparts; this phenomenon is widely referred to as the Urban Heat Island (UHI) (Arnfield, 2003). The adverse effects associated with the UHI phenomenon are extensively documented in the literature (Hassid et al., 2000). For example, urban dwellers are likely to experience increased thermal stress relative to rural dwellers. In extreme instances, these thermal stresses result in a high number of heat-related fatalities in urban areas, especially among the elderly and those with compromised immune systems (Goggins et al., 2012; Basu, 2002, 2009). Moreover, there have been reports of potential synergistic interactions between UHI and heat waves (Li and Bou-Zeid, 2013; Zhao et al., 2018; Founda and Santamouris, 2017; Khan et al., 2020), which may exacerbate mortalities in vulnerable

demographics (e.g., the elderly) and which are increasingly linked to respiratory health conditions (Paravantis et al., 2017; Kouis et al., 2019). In addition, the thermal discomfort caused by warmer temperatures in urban areas necessitates the use of energy-consuming mechanical equipment for space cooling in buildings, which subsequently and significantly contributes to increased building energy consumption in urban areas, especially during the summertime (Hassid et al., 2000; Kolokotroni et al., 2006).

Besides the issue of UHI, which, as we explain above, is a by-product of drastic land-use changes caused by rapid urbanization, rapid urbanization is also primarily linked to the worsening state of air quality in urban areas (Ling and Ting, 2010). This issue of air quality in urban areas is more or so tied to the increase in rural to urban migration and urban sprawls seen over the recent years. For example, Baklanov et al. report that megacities (i.e., population > 10 million) have increased from 2 cities in the 1970s to 23 cities in 2014 and this number is projected to increase to 37 cities in 2025 (Baklanov et al., 2010). Such drastic increases in urban populations result in increased anthropogenic activities such as fossil fuel combustion for vehicular usage, cooking and cooling or heating purposes in buildings which in turn increase the concentrations of air pollutants such as Sulphur dioxide (SO₂), Nitrogen

* Corresponding author.

E-mail address: ggyun@khu.ac.kr (G.Y. Yun).

dioxide (NO_2), Carbon monoxide (CO) and particulate matter (PM). These primary pollutants have significant contributions to the poor air quality found in urban areas and often lead to a myriad of health conditions, particularly respiratory and pulmonary diseases (Ghanbari Ghzikali et al., 2016; Olmo et al., 2011; Khaniabadi et al., 2017). Moreover, under specific natural conditions, primary air pollutants develop into secondary air pollutants such as ozone (O_3), which are themselves harmful to human health (Olmo et al., 2011).

In the perspective of urban environments, therefore, urban areas face two challenging problems that are parallel in nature but yet with compelling potential synergetic interactions; UHI and air pollution. For instance, on the one hand, high temperatures resulting from UHI in urban areas increase turbulent mixing and thus propelling air particles to higher boundary atmospheric levels. On the other hand, low ambient temperatures induced by the morbid absorption of short-wave radiation in urban areas during the day are likely to decrease the turbulent mixing and mixing layer height, both of which affect the concentrations and the vertical level at which the air pollutants exist. Fallmann et al., (2014) found that decreased mixed layer height was associated with increased near-surface concentrations of PM10. Similarly, (Swamy et al. (2017)) found that episodes of high SO_2 and PM10 in Kuwait were associated with meteorological conditions that induce low mixed layer heights. Conversely, the presence of high concentrations of air pollutants could also influence the manifestation and intensity of UHI in urban areas. For example, the presence of atmospheric aerosols could entrap long-wave radiation attempting to escape through the urban boundary layer and thus exacerbating the intensity of UHI. At the same time, increased particulates in urban areas could also promote urban cooling through radiative forcing mechanisms by reflecting incoming solar radiation to the atmosphere before reaching urban surfaces (Cao et al., 2016).

The above examples that demonstrate potential synergetic interactions between UHI and urban air pollution warrant the need for integrative studies that consider synergies and correlations between UHI and urban air pollution. Such studies are essential in developing coherent mitigative strategies that consider both improved air quality and thermal environments in urban areas. Consequently, this area of research constitutes a promising and worthy direction in urban climate research (Baklanov et al., 2010). One such a study has been conducted in Berlin during the summertime and they show that near-surface urban pollution index is negatively correlated with atmospheric UHI ($r = 0.31$). This relationship was more pronounced for nocturnal UHI than daytime UHI. At the same time, Surface UHI was associated with atmospheric air pollution index ($r = 0.62$), suggesting highly complex interactions between the two elements (i.e., UHI and air pollution) (Li et al., 2018).

Similarly, (Lai and Cheng (2009)) studied the associations between air quality and UHI under diverse synoptic weather patterns in a metropolitan area in China; they reported positive and statistically significant correlations between UHI and conventional air pollutants (i.e., NO_2 , CO, SO_2 and Particulate Matter) except for O_3 which showed a negative correlation with UHI potentially due to the photochemical reactions between NO_2 and oxygen that take place during the day. (Yoshikado and Tsuchida (1996)) explored the influence of UHI on air quality in a small coastal area in Japan during the wintertime. They report a convergence of high concentration of air pollutants attributed to UHI and thus attesting to the major effect of UHI on atmospheric airflow despite the increased ventilation in coastal cities resulting from the sea breeze. A similar study conducted in Paris (Serrat et al., 2006) also illustrates the potential effect of UHI on the availability and spatial distribution of air pollutants, mainly due to the influence of UHI on atmospheric turbulence. These studies provide scientific precedence for studying the interactions between UHI and air quality in megacities and urbanized areas. However, it is essential to note that the said interactions between UHI and air quality are influenced or exacerbated by other factors, including geographical location, level of urbanization, prevailing weather conditions, etc. Consequently, studies dealing with

such interactions should be contextualized to the area of interest. To the best of our knowledge and despite the recent intense debates surrounding increased warming and deteriorated air quality in Seoul, there has not been any attempt to explore the potential interactions between the UHI phenomenon and air quality in Seoul city so far.

Moreover, some of the crucial factors that influence both the availability and manifestation of UHI and air quality (e.g., population, land-use change) change over time and the interactions between UHI and air quality should, therefore, be based on the most recent available data and information. To that end, we attempt to explore the interactions between UHI and air pollutants in Seoul, South Korea. We use in-situ data of air temperature and air pollutants (i.e., SO_2 , NO_2 , O_3 , PM10, PM2.5) collected from automatic weather stations (T-AWS) and air pollution stations (AS) respectively. The T-AWS and AS are located in the center of Seoul and the data used in our study is for a period of nine years (i.e., 2009–2017).

Exploring the correlation between UHI and air pollution is important because it could result in coherent mitigation strategies for both UHI and air pollution, which are dominant issues in the context of urban studies. Moreover, such correlations are likely to be area-specific and our results provide a foundation for (I) future studies related to the interdependency between urban warming and air quality in Seoul (II) discussions on integrated mitigation strategies for urban warming and air quality in Seoul.

2. Methods

2.1. Study area

The study area is Seoul city, the capital and largest city in South Korea. It is located at a longitude of 126.59 E and latitude of 37.34 N in the central-western part of the Korean Peninsula. Seoul harbors a population of 25 million on a surface area of 605.25 km², making it one of the most densely populated cities in the world (Anon, 2020). Moreover, in the effort to provide sufficient infrastructure for the said population, Seoul has experienced explosive urbanization involving extensive land-use changes; this has made Seoul vulnerable to UHI-induced warming (Chung et al., 2004; Kug and Ahn, 2013). Also, Seoul experiences declining air quality owing to the diverse anthropogenic activities (e.g., vehicular use for transportation and heating and cooling in buildings) (Lee and Son, 2016). These factors make Seoul the ideal candidate to explore the potential interactions between UHI and air quality.

2.2. In-situ observation data of air temperature and air pollutants

The in-situ temperature measurements were collected from AWS located in Seoul. The T-AWS are operated through a cooperation between the Korean Meteorological Agency and the Seoul central metropolitan office. The temperature sensors at each AWS use metallic systems with thin films to sense hourly ambient temperatures in the ranges between -40 °C and 60 °C with an accuracy of ± 0.3 °C. The air pollution measuring stations are operated by the center for air quality integration and analysis at the institute for health and environment in Seoul. They measure common air pollutants found in dense urban areas, which include hourly recordings of SO_2 , NO_2 , CO, O_3 , PM10, and PM2.5. The sensors use ultraviolet photometry methods for SO_2 and O_3 in the ranges between 0 – 1 ppm. Non-dispersive external analysis is used to measure CO in the ranges 0–50 ppm and beta-ray absorption methods are used for estimating PM in the ranges 0–5000 $\mu\text{g}/\text{m}^3$. There are currently 54 T-AWS for meteorological weather measurements and 25 Automatic Stations (AS) for air pollution measurements in Seoul city. However, for this study, only 7 T-AWS and 6 AS were considered; this is because we needed to identify AWS and AS in close proximity to each other to accurately estimate the interactions between temperature (e.g., UHI levels) and air pollution. The distance between each AWS and the

associated AS was approximately 0.5 km or less. In some instances, data from one AS overlapped with two T-AWS in that air pollution data from a single AS was compared with temperature measurements from two different T-AWS. Table 1 and Table 2 show the information on the considered 6 AS and 7 AWS, respectively while Table 3 shows the specific methods used in monitoring air temperature and air pollutant concentrations. Additionally, Table 4 shows physical characteristics surrounding each T-AWS while Fig. 1 shows the locations of the considered AWS and AS within Seoul city.

2.3. Data processing

We used a large dataset (i.e., 551,880 data entries) of air temperature and air pollution recorded for a period of nine years (i.e., 2009–2017) from seven T-AWS and six AS located in the middle of Seoul. With such large datasets, it is somewhat inevitable to find errors and inconsistent recordings that can be primarily attributed to failure or improper calibration of the equipment. If left untreated, such recordings are likely to negatively affect the outcome of a given statistical analysis. Consequently, we conducted several tests to identify potentially wrong recordings and eliminate them from our datasets. We conducted range tests, step tests, as well as persistence tests. Range tests ensure that the recordings are within logical ranges. Step tests check for outliers in the dataset; for example, rapid temperature changes within a short time interval (e.g., above 8 °C) were considered outliers as such temperature changes are highly unlikely within short time intervals. Persistent tests involved identifying recordings that are constant for long periods. Such recordings were also removed from the dataset as they likely resulted from equipment failure. A detailed explanation of the above tests (i.e., range, step and persistence tests) conducted to identify erroneous data in our dataset is given by Estevez et al., (Estévez et al., 2011)

2.4. Calculating urban heat island intensity (UHII)

UHI is quantified using multiple indices based on either land surface temperature or air temperature. In the current study, we employed an air-based UHI index, the Urban Heat Island Intensity Index (UHII), which is merely the difference in temperature between the ambient air temperature of a specific urban area and that of a representative rural or suburban area. The area chosen to represent rural/suburban areas is of paramount importance; when improperly chosen, it poses a risk of incorrect assessments of UHI and its subsequent effects (Runnalls and Oke, 2000). To prevent improper estimates of UHI associated with the poor selection of representative rural areas, the World Meteorological Agency (WMA) proposes guidelines for the proper selection of representative urban areas (Oke, 2020). For instance, representative rural areas should be located in vegetated areas on flat terrain. Common choices include airport stations or clear fields used for farming purposes away from major infrastructure such as tall buildings and bridges (Hamdi and Schayes, 2008). Following such guidelines, the Neunggok weather station, which also shares the same latitude with central Seoul and has previously been remarked as a representative rural area by UHI studies in Seoul (Lee et al., 2016; Oh et al., 2020), was selected as our reference station and UHII ultimately calculated as in the equation below.

Table 1
Geographical location and land use information of the AS (Air pollution stations).

| Station [AS] | Latitude | Longitude | Land use |
|--------------|----------|-----------|------------------|
| 1 | 37.51 | 127.04 | Residential area |
| 2 | 37.54 | 126.83 | Residential area |
| 3 | 37.58 | 127.09 | Residential area |
| 4 | 37.52 | 126.89 | Industrial area |
| 5 | 37.61 | 126.93 | Residential area |
| 6 | 37.54 | 127.04 | Industrial area |

Table 2

Geographical location and land use information of the T-AWS (Temperature automatic weather stations).

| Station [T-AWS] | Latitude | Longitude | Land use | Nearby AS |
|-----------------|----------|-----------|------------------|-----------|
| 1 | 37.51 | 127.04 | Residential area | 1 |
| 2 | 37.55 | 126.84 | Residential area | 2 |
| 3 | 37.58 | 127.08 | Residential area | 3 |
| 4 | 37.52 | 126.90 | Industrial area | 4 |
| 5 | 37.51 | 127.04 | Industrial area | 1 |
| 6 | 37.53 | 127.04 | Residential area | 6 |
| 7 | 37.60 | 126.92 | Residential area | 5 |

Table 3

Air temperature and air pollutant monitoring methods used at the observation stations.

| Element | Method | Range | Accuracy |
|-----------------|----------------------------------|------------------------------|-------------------------|
| Air temperature | Metallic system with thin films | -40 °C – 60 °C | ± 0.3 °C |
| SO ₂ | Ultraviolet photometry | 0 ppm – 1 ppm | ± 0.0004 ppm |
| NO ₂ | Ultraviolet photometry | 0 ppm – 1 ppm | ± 0.0004 ppm |
| CO | Non-dispersive external analysis | 0 ppm – 50 ppm | ± 0.0004 ppm |
| O ₃ | Ultraviolet photometry | 0 ppm – 1 ppm | ± 0.0004 ppm |
| PM10 and PM2.5 | Beta-ray absorption | 0 ppm – 50 µg/m ³ | ± 0.4 µg/m ³ |

Table 4

Physical characteristics surrounding each T-AWS.

| Station [T-AWS] | Sky view factor | Green area [%] | Road area [%] | Building area [%] | Bare area [%] | Impervious area [%] |
|-----------------|-----------------|----------------|---------------|-------------------|---------------|---------------------|
| 1 | 0.86 | 9.1 | 23.1 | 38.5 | 7.9 | 61.6 |
| 2 | 0.79 | 34.6 | 18.5 | 16.0 | 9.6 | 34.4 |
| 3 | 0.96 | 2.3 | 18.1 | 52.3 | 5.9 | 70.4 |
| 4 | 0.79 | 19.2 | 40.2 | 14.3 | 4.9 | 54.2 |
| 5 | 0.85 | 14.8 | 39.3 | 23.5 | 1.0 | 62.9 |
| 6 | 0.78 | 14.8 | 12.9 | 21.3 | 11.9 | 34.1 |
| 7 | 0.81 | 9.9 | 15.1 | 45.7 | 7.9 | 60.8 |

$$UHII = T_{urban} - T_{rural} \quad (1)$$

Where *UHII* is urban heat island intensity [°C], *T_{urban}* is the ambient temperature of an urban area [°C] and *T_{rural}* is the ambient temperature of a representative rural area

2.5. Data analysis

To better understand the potential interactions between UHI and air quality in Seoul, we first studied temporal manifestations of both elements in terms of annual, monthly, seasonal and daily trends for the entire period (2009–2017). Yearly trends were calculated as the average monthly values for each year resulting in 1 value per year. Monthly trends were computed as the average of the maximum values for each month in the dataset resulting in 1 value for each month and a total of 12 values representing the months of the year. Seasonal trends were computed based on the four climatic seasons experienced in Seoul city; summer, winter, autumn and spring. Summer and winter take place from June to August and December to February, respectively. Spring and autumn take place from March to May and September to November, respectively. Consequently, seasonal trends were computed as monthly averages for each season.

Diurnal trends were calculated as the average value for each hour

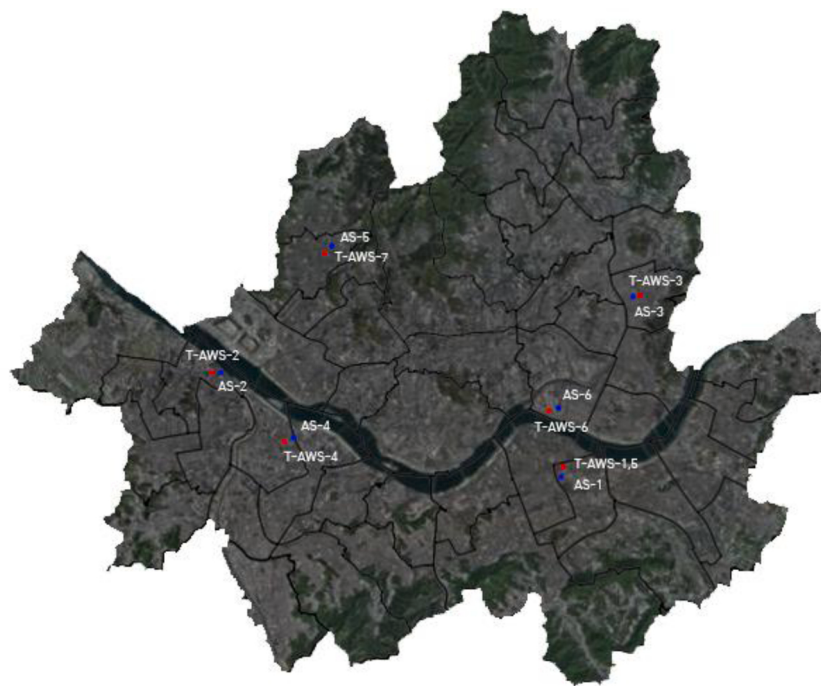


Fig. 1. Locations of the considered AWS and AS.

within the dataset. For example, the entire dataset was arranged so that all the values of UHI/air pollutants at midnight (i.e., 0 h) for the whole time-series period (i.e., 2009–2017) were grouped in a single cluster and their average computed. The same was done for all UHI/air pollutant values at each hour, resulting in 24 values representing the 24 h of the day. These are standard methods commonly used to extract meaningful correlations from large datasets and have been previously employed in several UHI-related studies (Arifwidodo and Tanaka, 2015; Yun et al., 2020). Fig. 2 below illustrates the conducted process.

To explore the potential relationship between UHII and air pollution levels while minimizing the influence of minor observation errors, the UHII data was quantized into bins. The bins were based on 1 °C width intervals resulting in a total of eleven UHII categories. We then calculated the mean value of each air pollutant for each of the eleven UHII bins. To assess if the mean differences in air pollution concentrations among the eight bins were statistically significant, we employed the Analysis of variance test (ANOVA). ANOVA reveals whether the mean differences among many different groups/categories are statistically significant by

analyzing the variance among the groups; for a set of n-values [$X_1, X_2, X_3, \dots, X_n$], the variance is computed as a quotient of the sum of squares and degrees of freedom (See Eq. 2). We also conducted a regression analysis to gauge the strength of correlations between UHI levels and air pollutant concentrations. Also, to explore the potential influence of short-term anthropogenic activities on the relationship between UHI and air pollution in Seoul, we studied the correlations between UHII and air pollutant concentrations levels separately for weekdays when anthropogenic activities are high and weekends when anthropogenic activities are often low. Weekdays were considered as Monday through to Friday, while weekends were considered as Saturday and Sunday. Similarly, to gauge the likely effect of land-use on the interaction between UHI and air pollution, the interactions between UHII and air pollutant concentration levels were assessed individually for the monitoring stations located in residential areas and those located in industrial areas.

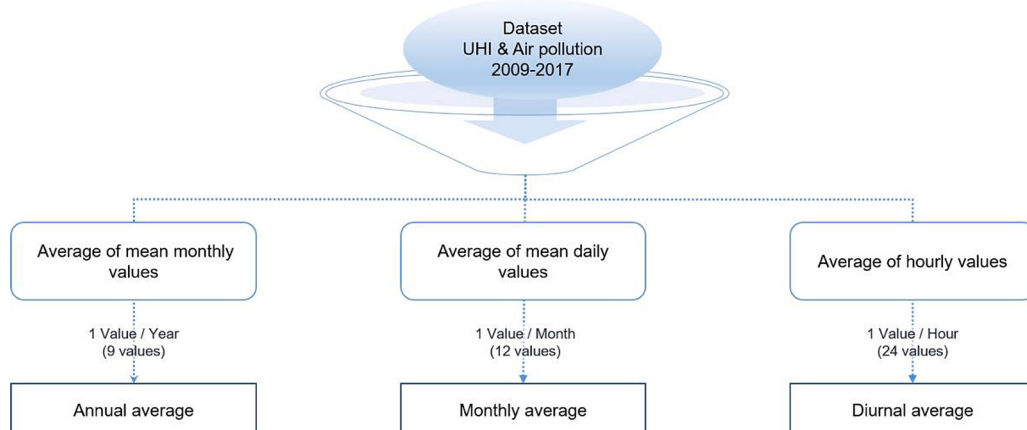


Fig. 2. Process for calculating annual, monthly and diurnal averages.

$$\text{Variance} = \sqrt{\frac{\sum_{i=1}^n (x_i - \bar{x})^2}{n - 1}} \quad (2)$$

Where n is the number of observations, x_i is the observed value and \bar{x} is the sample mean. The statistical significance for the ANOVA test and the regression analysis was determined at a p-value < 0.001. The assumption of normality was evaluated using the "Skewness" and "Kurtosis" criteria. "Skewness" and "Kurtosis" values between -1 and 1 generally indicate that the data is normally distributed around the mean (Mardia, 2020). This same criterion was employed in our study.

3. Results and discussion

Table 5 shows the descriptive statistics of our dataset upon the completion of the data processes described in section 2.3. As shown in the table, the Mean (M) UHII value for the entire dataset (i.e., 2009–2017) was 1.6 °C, which is relatively substantial. Similarly, substantial amounts of air pollutants were observed in the period considered. Our analysis shows that UHII gradually increased from 2009 to 2012, after which constant levels of UHII were experienced from 2013 to 2017. The annual mean tended to fluctuate between 0.8 °C in 2009 and 2 °C in the years between 2013 and 2017. The lowest mean value of UHII was observed in 2009 (M = 0.85, SD = 1.69) and the highest mean value was observed in 2017 (M = 2.02, SD = 1.65).

In regards to SO₂, the annual changes in mean values showed no definite trends over the years. However, the temporal trend analysis shows small gradual increases fluctuating between the lowest observed concentration levels (M = 0.0043, SD = 0.00199) in 2011 and the highest observed concentration levels in 2014 (M = 0.0053, SD = 0.00162) except for the year 2016 which experienced abnormally high annual mean SO₂ concentration levels (M = 0.00151, SD = 0.0015). CO concentration levels were observed to be relatively constant over the entire period and tended to demonstrate no particular trend; the mean concentration levels tended to fluctuate slightly from year to year. The highest mean concentration of CO was observed in 2011 (M = 0.4887 ppm, SD = 0.2084 ppm) and the lowest in 2014 (M = 0.467 ppm, SD = 0.2033 ppm). Our results are in agreement with those reported by Kim et al., (Kim et al., 2015), which studied long term trends in CO concentration levels in Seoul city (i.e., from 1989 to 2013). Annual mean values of NO₂ concentrations were observed to generally decrease or, in some years, show slight increases by levels below 0.021 ppm.

The concentrations of PM10 and PM2.5 tended to show no substantial variations over the years. For instance, the highest mean annual value of PM2.5 (M = 24.1186 µg/m³, SD = 12.0574) was observed in 2016 and the lowest mean annual value (M = 20.5098 µg/m³, SD = 11.9381) was observed in 2012. Similar annual trends were seen for the PM10 data where the highest mean value in the considered period was 46.4737 µg/m³ (SD = 21.5343) also observed in 2016 and the lowest value was 38.8885 µg/m³ (SD = 20.9159) also observed in 2012 suggesting positive correlations between the two elements. In regards to ground-level ozone, we observed slight but gradual increases in annual

mean values of ozone except for the year 2009, which showed 0.0022 ppm higher than the succeeding year of 2010. For the rest of our study period, however, the trend gradually increased with the lowest mean value observed in 2010 (M = 0.0168 ppm, SD = 0.0145) and the highest mean value observed in 2017 (M = 0.0217 ppm, SD = 0.0157). **Fig. 3** shows the annual trends in Seoul's UHI and air pollutants in the period 2009–2017.

The consistent reductions in temporal emissions of SO₂, NO₂, CO can be attributed to technological improvements and regulatory initiatives by the Korean government (e.g., the use of alternative fuels with low sulfur contents) (Kim et al., 2015) whereas the increase in O₃ emissions can be attributed to the decrease in O₃ precursors (i.e., CO and NO₂) which result in the reduced destruction of O₃ via the titration process (Swamy et al., 2017) (See Eq. 3–5 below). This theory is supported by several previous studies that observed increased concentrations of ground-level ozone in Seoul city. Other studies have attributed the elevated levels of O₃ to convective activities that promote long-range transport of ozone from neighboring countries (Oh et al., 2010; Kottmarthi and Carmichael, 1990).



3.1. Potential interactions between Seoul's UHI and air pollutants

We attempted to assess the potential interactions between UHI and air pollutant concentrations in Seoul. To extract clear patterns from our large dataset while ignoring the influences of minor observation errors, we binned UHI data into clusters of 1 °C intervals resulting in 11 groups of UHI; the minimum UHI level was -3.10 °C and the maximum was 6.30 °C. We then calculated the mean values for the air pollutants corresponding to each UHI bin. **Table 6** demonstrates potential interactions between UHI and the air pollutants considered in our study (i.e., NO₂, CO, O₃, SO₂, PM10, and PM2.5).

Generally, our results show that UHI in Seoul is highly correlated with air pollution concentrations. For example, different clusters of UHI levels showed differences in mean SO₂ concentrations; SO₂ concentrations tended to increase with increasing UHI suggesting a potential interaction between UHI and SO₂ concentrations. An increase in UHI levels by 1 °C tended to indicate a 0.001 ppm increase in SO₂ concentration. Also, a follow-up ANOVA analysis showed statistically significant differences among the different clusters of UHII; F (1,074,259) = 46.108, P-value < 0.001. Similarly, NO₂ mean concentration levels tended to increase with an increase in UHI concentrations. The mean differences among the UHI groups were also statistically significant, F (1,074,259) = 556.393, P-value < 0.001. The same positive trends were observed between CO and UHI; the mean differences in CO concentration levels tended to increase with increasing UHI levels and the said differences were statistically significant, F (1,074,259) = 332.467, P-value < 0.001. The mean concentration levels of PM10 also tended to show statistically significant differences among the UHI categories, F (1,074,259) = 127.815, P-value < 0.001. Similar positive correlations were observed between PM2.5 and UHI, F (1,074,259) = 127.815, P-value < 0.001. Surprisingly, however, the mean concentrations values of O₃ tended to decrease with increasing UHI levels. The differences in mean concentrations of O₃ among the different UHI groups were also statistically significant, F (1,074,259) = 503.896, P-value < 0.001.

Conclusively, therefore, there exists a relationship between UHII and air pollutants and in most cases, the strength of these relationships tended to vary across types of air pollutants. From our results, we found the strongest relationship to be between UHII and SO₂ ($R^2 = 0.775$) and UHII and O₃ ($R^2 = 0.738$) despite the relationship between O₃ and UHII being negative. There was also a medium-strength relationship between

Table 5
Descriptive statistics of the dataset.

| variable | Data description | | | | |
|----------------------------|------------------|---------|---------|--------|--------|
| | N | Minimum | Maximum | Mean | SD |
| UHII [°C] | 74,270 | -3.100 | 6.300 | 1.685 | 1.769 |
| SO ₂ [ppm] | 74,270 | 0.001 | 0.009 | 0.052 | 0.002 |
| NO ₂ [ppm] | 74,270 | 0.010 | 0.076 | 0.035 | 0.016 |
| CO [ppm] | 74,270 | 0.100 | 1.043 | 0.452 | 0.189 |
| O ₃ [ppm] | 74,270 | 0.010 | 0.066 | 0.019 | 0.016 |
| PM10 [µg/m ³] | 74,270 | 11.000 | 101.000 | 48.153 | 22.166 |
| PM2.5 [µg/m ³] | 74,270 | 12.000 | 55.000 | 23.438 | 12.819 |

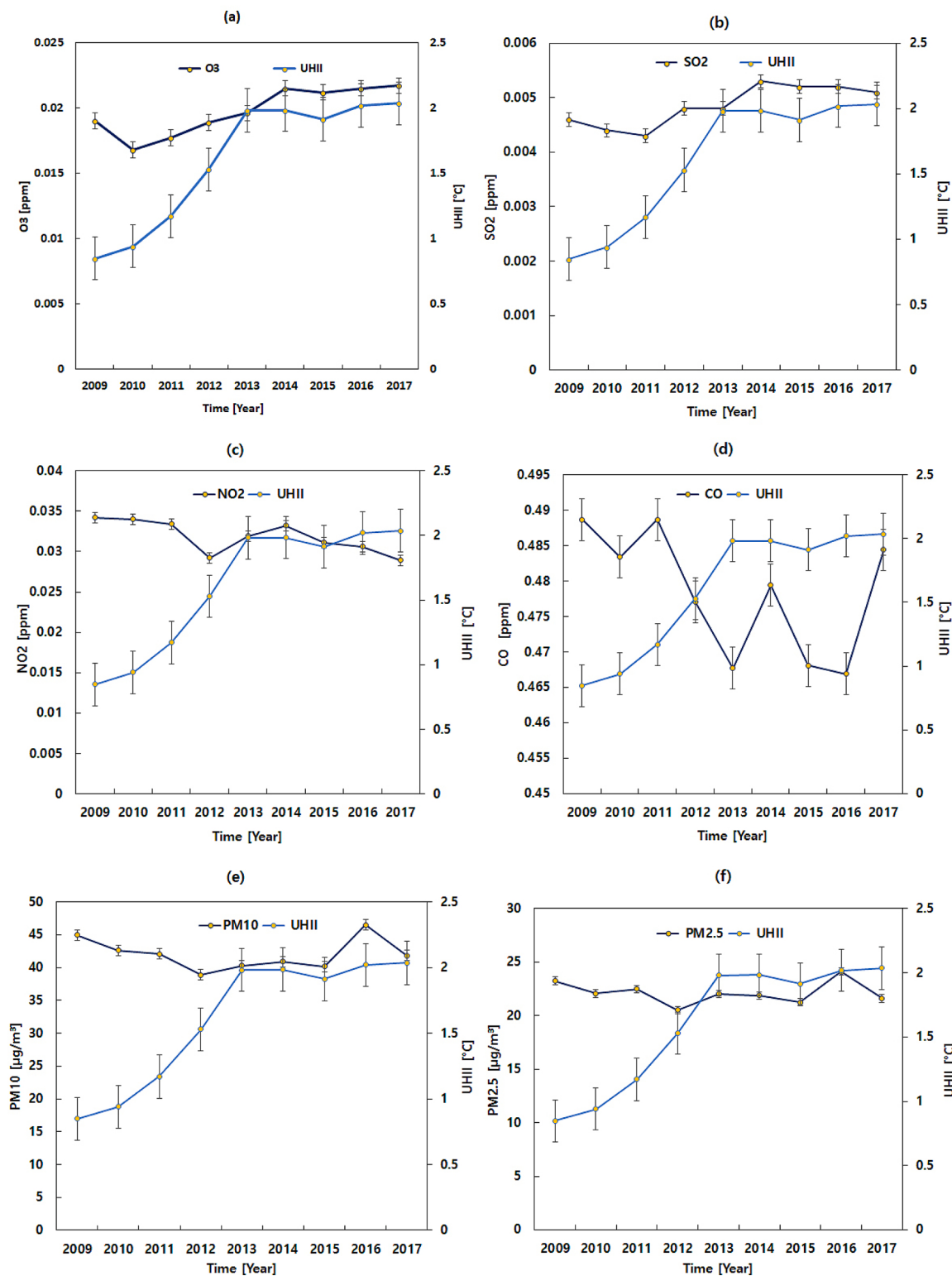


Fig. 3. Annual trends between UHII and air pollutants for the period 2009 – 2017 (a) O₃ (b) SO₂ (c) NO₂ (d) CO (e) PM10 (f) PM2.5.

PM10 ($R^2 = 0.628$) and NO₂ ($R^2 = 0.558$). The relatively weak relationships were observed between PM2.5 ($R^2 = 0.492$) and CO ($R^2 = 0.441$).

Our results are consistent with previous studies (Lai and Cheng, 2009; Fallmann et al., 2016), which show that generally, primary pollutants such as NO₂, CO, SO₂, PM10 and PM2.5 increase with increasing near-surface air temperature (i.e., increasing UHI levels). This increase in primary pollutants is potentially due to the earlier discussed potential

effect of UHI on the mixing layer height; while the mixing layer is affected by several factors (e.g., wind velocity, relative humidity) (Dandou et al., 2009), changes in the thermal composition of urban atmospheres have significantly complex influences on the atmospheric structure and may result in reduced vertical mixing and thus increasing the net surface concentrations of most primary air pollutants (Yassin et al., 2018). However, the negative correlations between increased UHI levels on the mean concentrations of ozone can be attributed to the

Table 6

Changes in mean air pollutant concentrations under different UHII conditions.

| UHI levels (°C) | | | | | | | | | | | Correlations | |
|----------------------------|--------------|----------------------|----------------------|----------------------|---------------------|--------------------|--------------------|--------------------|--------------------|--------------------|--------------------|---------|
| | Level1 | Level2 | Level3 | Level4 | Level5 | Level6 | Level7 | Level8 | Level9 | Level10 | Level11 | |
| SO ₂ (ppm) | UHII ≤ -3.10 | -3.09 ≤ UHII ≤ -2.10 | -2.09 ≤ UHII ≤ -1.10 | -1.09 ≤ UHII ≤ -0.10 | -0.09 ≤ UHII ≤ 0.90 | 0.91 ≤ UHII ≤ 1.90 | 1.91 ≤ UHII ≤ 2.90 | 2.91 ≤ UHII ≤ 3.90 | 3.91 ≤ UHII ≤ 4.90 | 4.91 ≤ UHII ≤ 5.90 | 5.91 ≤ UHII ≤ 6.90 | |
| | 0.0046 | 0.0051 | 0.0052 | 0.0051 | 0.0051 | 0.0051 | 0.0052 | 0.0053 | 0.0054 | 0.0055 | 0.0057 | |
| | ± | ± | ± | ± | ± | ± | ± | ± | ± | ± | ± | 0.775* |
| | 0.002 | 0.002 | 0.002 | 0.002 | 0.002 | 0.002 | 0.002 | 0.002 | 0.001 | 0.001 | 0.001 | |
| | 0.0188 | 0.027 | 0.0243 | 0.0229 | 0.0222 | 0.0207 | 0.0172 | 0.0133 | 0.0119 | 0.0117 | 0.0116 | |
| | ± | ± | ± | ± | ± | ± | ± | ± | ± | ± | ± | -0.738* |
| | 0.015 | 0.019 | 0.018 | 0.016 | 0.016 | 0.017 | 0.017 | 0.014 | 0.013 | 0.013 | 0.012 | |
| | 0.0368 | 0.0354 | 0.0343 | 0.0326 | 0.031 | 0.0321 | 0.0361 | 0.0395 | 0.0425 | 0.0445 | 0.0479 | |
| | ± | ± | ± | ± | ± | ± | ± | ± | ± | ± | ± | 0.558* |
| | 0.015 | 0.016 | 0.015 | 0.015 | 0.015 | 0.015 | 0.016 | 0.017 | 0.017 | 0.017 | 0.018 | |
| O ₃ (ppm) | 0.4649 | 0.4839 | 0.4596 | 0.4294 | 0.4133 | 0.4265 | 0.4643 | 0.5009 | 0.5187 | 0.528 | 0.5547 | |
| | ± | ± | ± | ± | ± | ± | ± | ± | ± | ± | ± | 0.441* |
| | 0.206 | 0.300 | 0.192 | 0.181 | 0.174 | 0.176 | 0.189 | 0.202 | 0.204 | 0.202 | 0.209 | |
| | 39.00 | 45.33 | 43.45 | 40.33 | 40.13 | 41.91 | 45.29 | 46.91 | 47.23 | 47.59 | 50.79 | |
| PM10 (µg/m ³) | ± | ± | ± | ± | ± | ± | ± | ± | ± | ± | ± | 0.628* |
| | 22.645 | 22.271 | 23.394 | 22.469 | 22.195 | 21.653 | 21.97 | 21.663 | 21.765 | 21.355 | 21.613 | |
| | ± | ± | ± | ± | ± | ± | ± | ± | ± | ± | ± | 0.492* |
| PM2.5 (µg/m ³) | 23.56 | 24.69 | 22.93 | 21.14 | 21.60 | 22.96 | 24.97 | 25.81 | 25.82 | 25.98 | 27.61 | |
| | ± | ± | ± | ± | ± | ± | ± | ± | ± | ± | ± | |
| | 14.052 | 12.218 | 12.993 | 12.354 | 12.519 | 12.668 | 12.997 | 12.892 | 12.676 | 12.771 | 13.571 | |

Statistically significant results are marked with an asterisk symbol (*). Statistical significance is determined at P < 0.001).

titration effect shown earlier in Eqs. 3,4 and 5. On the one hand, the presence of high levels of radiation during the day facilitates the photochemical reaction among O₃ precursors inducing high concentrations of O₃. On the other hand, urban materials that are often characterized by high solar absorptance capacities tend to store the incoming short wave solar radiations reducing atmospheric UHI. These two separate mechanisms result in increased O₃ concentrations and reduced UHI during the day. At night, the O₃ concentrations are exhausted by NO through reverse chemical reactions (refer to Eqs. 3,4 and 5) while, at the same time, the heat absorbed during the day is emitted as longwave radiation increasing the UHI. These two separate mechanisms result in low ozone concentrations and conversely increased atmospheric UHI at night and hence the negative correlation between UHI and mean concentration levels observed in the current study.

The obtained results have broad implications regarding the mitigation strategies employed in urban areas to counter the earlier discussed effects of UHI and air pollution. Ideally, since the two issues (i.e., UHI and air pollution) tend to co-exist in urban areas and since they show potential interactions, mitigation techniques that provide coherent solutions to both issues simultaneously would be preferable. Akbari et al., (Akbari et al., 2016) give an extensive review of commonly employed mitigation strategies for UHI. Some of these strategies can be optimized to reduce UHI while simultaneously decreasing the dispersion of air pollutants, while some other strategies can exacerbate air quality conditions. For example, while highly reflective roofs and walls can mitigate UHI through the reflection of incoming shortwave solar radiation during the day and thereby reducing heat absorption and subsequently heat storage, the reflected short-wave radiation can facilitate photochemical reactions needed for ozone formation and thereby increasing daytime ozone concentration levels. Furthermore, other UHI mitigative strategies such as increased vegetation, trees and overall greenery in urban areas are likely to influence the turbulent flows and circulation patterns of urban air which could also influence the dispersion and distribution of air pollutants particularly through the modification of the mixing-layer height in the urban boundary canopy (Fallmann, 2014).

3.2. Potential interactions between Seoul's seasonal UHI and air pollutants

To efficiently explore the potential interactions between UHI and air pollutants based on seasons, we first explore the monthly manifestations

of UHI and the distribution of air pollutants. Fig. 4 shows the monthly trends in the intensity and concentration of air pollutants in Seoul. In regards to UHI and for the period considered (i.e., 2009–2017), the highest mean monthly UHII was observed in October (M = 2 °C, SD = 1.90 °C) while the lowest mean monthly UHII was observed in July (M = 1.1 °C, SD = 1.2 °C). Generally, UHII was relatively higher during the autumn and winter months than in the spring and summer months. Such seasonal behavior of UHI can be explained by the known interactions between UHI and synoptic weather conditions. It is well established that the intensity of UHI tends to be more pronounced in conditions characterized by low winds, clear skies and low relative humidity (Liu et al., 2007). Specifically, the influence of humidity and precipitation on UHI has been extensively documented by several previous studies and the consensus from such studies is that UHI is negatively correlated with relative humidity (Borbora and Das, 2014; Kim and Baik, 2002). This is, possibly, because increased humidity is associated with increased rates of evaporation, which in turn result in reduced surface temperature through evaporative cooling mechanisms. Consequently, the reduced intensity of UHI in summertime observed here is attributable to the high relative humidity common in Korean summers and is consistent with previous studies conducted in Seoul (Kim and Baik, 2002). At the same time, the observed increases in UHII during the wintertime can be attributed to increased anthropogenic activities such as space heating of buildings during the winter (Oke et al., 1991).

In regards to SO₂, generally, higher concentrations were observed during the winter and spring season than in the summer and autumn seasons. For example, the highest mean monthly value of SO₂ concentration levels in our study period was observed in February (M = 0.006 ppm, SD = 0.0016 ppm) and the lowest in August (M = 0.0039 ppm, SD = 0.00165 ppm). These observations are in agreement with previous studies in Seoul (Khan et al., 2017; Thi Nguyen and Kim, 2006) and Beijing (Lin et al., 2012). The low concentrations of SO₂ in the summertime and it's increasing in wintertime can be attributed to a combined effect of synoptic weather conditions and anthropogenic activities. The high precipitation and frequent temperature inversions associated with the summertime monsoon weather conditions promote the expansion of the mixing heights, thus resulting in reduced SO₂ concentrations (Perkauskas and Mikelinskienė, 2020). Conversely, the low precipitation levels seen in the wintertime can facilitate low mixing heights resulting in a build-up of SO₂ concentrations (Gupta et al., 2003). Seoul winters and spring periods are also dominated by strong

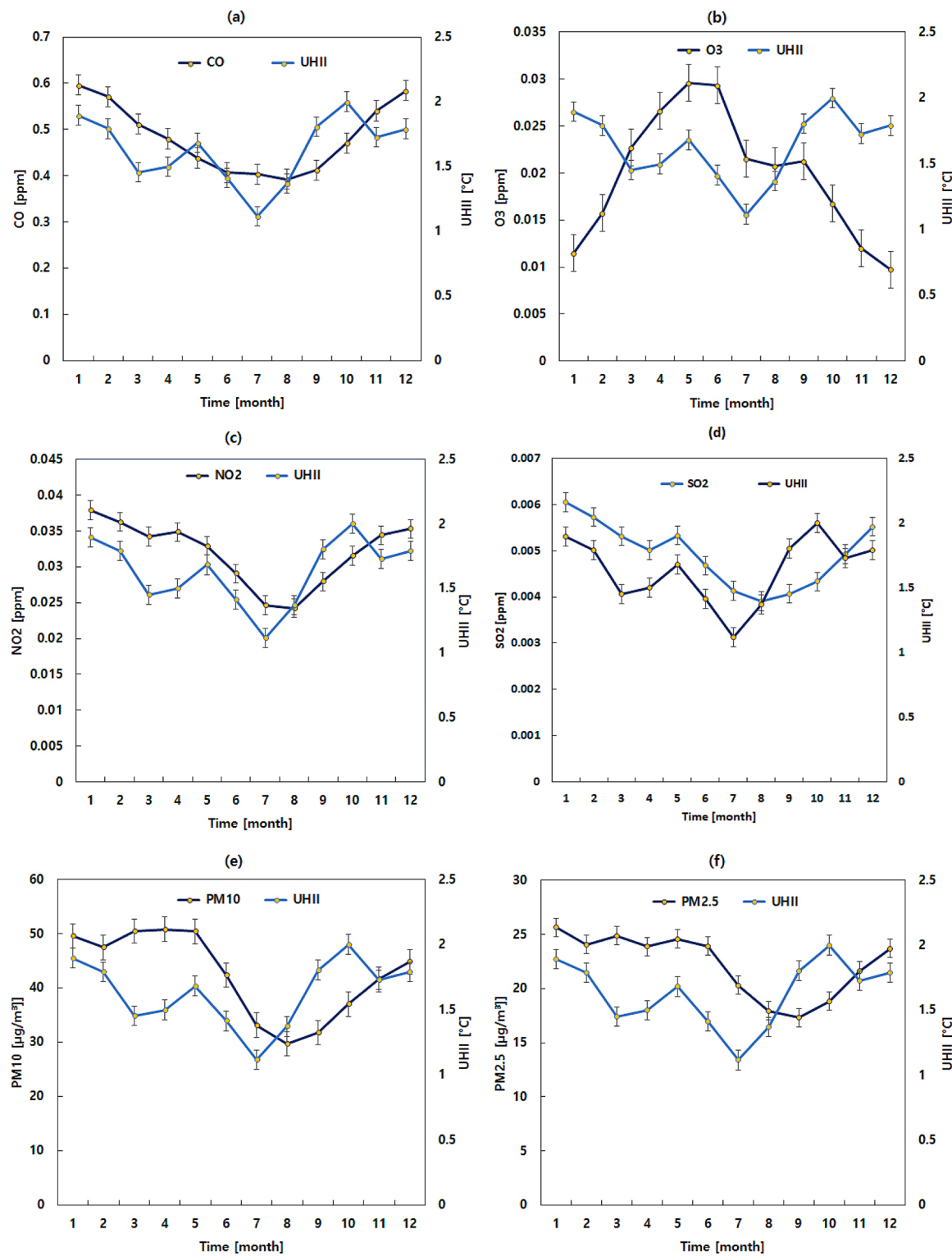


Fig. 4. Monthly trends in between UHII and air pollutants (a) CO (b) O₃ (c) NO₂ (d) SO₂ (e) PM10 (f).PM2.5

westerly winds that are likely to favor the long-range transport of SO₂ from external sources (Jeong et al., 2013). The low temperatures prevalent in winter and spring periods also encourage heating-induced anthropogenic activities that act as sources of SO₂ emissions (Feng et al., 2014).

Similar patterns were observed in the seasonal distribution of the other air pollutants studied here; NO₂, CO, PM10 and PM2.5 except for O₃. The lowest mean values of NO₂ ($M = 0.024 \text{ ppm}$, $SD = 0.01 \text{ ppm}$),

CO ($M = 0.391 \text{ ppm}$, $SD = 0.172 \text{ ppm}$), PM10 ($M = 29.680 \mu\text{g}/\text{m}^3$, $SD = 17.876 \mu\text{g}/\text{m}^3$) and PM2.5 ($M = 17.302 \mu\text{g}/\text{m}^3$, $SD = 10.890 \mu\text{g}/\text{m}^3$) were observed in August possibly due to the high precipitation during Korean summers that washes out atmospheric aerosols and thus reducing their concentrations (Loosmore and Cederwall, 2004; Choi et al., 2008). The highest mean values of NO₂, CO, PM10 and PM2.5 were observed in winter and spring season and are attributed to a combined effect of the low atmospheric boundary layer that causes

stagnant air conditions, absence of high-intensity sunlight necessary for reduction processes to take place and low precipitation that would otherwise result in an atmospheric cleansing effect (Ray and Kim, 2014). The high air pollutant concentrations observed in the spring season are also likely due to the Asian dust events that are common in the spring period (Kim and Kim, 2003; Lee et al., 2006). This demonstrates the potential inter-correlation between the individual air pollutants and possibly suggesting similar driving forces as those that influence the behavior of seasonal SO₂ (i.e., high precipitation during the summertime and increased anthropogenic activities during the wintertime). However, seasonal O₃ tended to show a pattern opposite to that of the other air pollutants; in general, O₃ tended to increase from spring through to autumn peaking in the summer months and decreasing again in winter. For example, the highest monthly mean value was observed in June ($M = 0.029$ ppm, $SD = 0.017$ ppm) while the lowest value was observed in December ($M = 0.0097$ ppm, $SD = 0.08$ ppm). This observed unique behavior demonstrated by O₃ is largely due to the increased temperatures in the summertime, which favor the active photochemical reactions necessary to produce O₃ from its precursors (e.g., NO₂) (Iqbal et al., 2014; Klumpp et al., 2006).

From the trends above and Fig. 4, UHI manifestation and the dispersion of air pollutants are largely influenced by seasonal changes. Consequently, we hypothesized that the interactions between UHI and air pollutants might vary depending on the season, particularly due to the temperature inversion phenomenon (Kahl, 1990). We thus conducted a linear regression analysis to explore interactions between UHI and air pollution based on the season of the year. We found a substantial seasonal effect on the strength of the relationship between UHII and air pollutant concentrations. Specifically, for SO₂, we found stronger correlations in winter ($R^2 = 0.84$, P -value < 0.001) and spring ($R^2 = 0.698$, $P < 0.001$) than in summer ($R^2 = 0.001$, P -value = 0.067) and Autumn ($R^2 = 0.228$, P -value = 0.079) suggesting stronger interactions between SO₂ and UHI under conditions that favor pronounced UHI. Similarly, we found stronger correlations between UHI and PM10 in winter ($R^2 = 0.590$, P -value < 0.001) and spring ($R^2 = 0.326$, P -value = 0.061) than in summer ($R^2 = 0.122$, $P = 0.072$) and Autumn ($R^2 = 0.126$, P -value = 0.088).

In contrast to SO₂ and PM10, the correlation between UHI and PM2.5 were stronger in autumn ($R^2 = 0.695$, P -value < 0.001) and summer ($R^2 = 0.294$, $P < 0.006$) than in spring ($R^2 = 0.216$, P -value = 0.013) and winter ($R^2 = 0.027$, P -value = 0.441). Similarly, stronger correlations were observed between UHI and O₃ in autumn ($R^2 = 0.512$, P -value < 0.001) and summer ($R^2 = 0.488$, P -value < 0.001) than in spring ($R^2 = 0.371$, $P = 0.02$) and winter ($R^2 = 0.12$, P -value = 0.097) while the correlations between UHI and CO and those between UHI and NO₂ were not statistically significant for all seasons.

Conclusively, therefore, the strongest relationships between UHII and the majority of the air pollutants (i.e., CO, NO₂, O₃, and PM2.5) were observed in autumn while those for PM10 and SO₂ were observed in winter. Conversely, the weakest relationships were observed in the summertime for CO, PM10 and SO₂ while those for NO₂, O₃ and PM2.5 were observed in wintertime. These results indicate that while the relationship between UHI and air pollutants in urban areas may be explained by already established mechanisms especially those pertaining to the UHI-induced changes in the thermal component of the urban climate, the said relationship may also be influenced by several other phenomena not established in the literature and thus warranting intensive future studies.

The obtained results regarding the seasonal effects on the interactions between UHI and air pollutant concentrations constitute a major finding of the current study. While similar studies in Beijing (Lai and Cheng, 2009), Tokyo (Yoshikado and Tsuchida, 1996) and Paris (Sarrat et al., 2006) on the relationship between UHI and air pollutant concentrations were conducted for specific seasons, we explore such relationships for multiple seasons and highlight the particular relationships in each season. For example, we show that the relationship

between UHI and air pollutant concentrations is weakest in the summertime, possibly due to the monsoon rains that are prevalent in Korea and which likely weaken the UHI effect and consequently the convergence of air pollutant concentrations. Table 7 shows the strongest and weakest relationships between UHII and air pollutants based on season, while Fig. 5 shows the general seasonal effect on the relationship between UHI and air pollutants.

Moreover, the seasonal effect on the relationship between UHI and common urban air pollutants observed here has broad implications regarding the UHI mitigative strategies. As we discussed earlier, on the one hand, UHI mitigative strategies such as the use of highly reflective urban materials could promote the formation of ozone increasing its concentrations. On the other hand, certain strategies such as those involving the reduction of anthropogenic heat fluxes could, although indirectly, serve to simultaneously reduce both UHI levels and air pollution (e.g., reduced air conditioning usage). These effects of UHI mitigative measures on the interactions between UHI and atmospheric air pollutants are likely to vary from season to season. Consequently, it is crucial that UHI mitigative strategies be optimized considering their potential influence on air pollutant concentrations and, at the same time, considering the seasonal effect. To do so, extensive scientific discussions are required to accurately quantify the said possible influences of UHI mitigative strategies on air pollutant concentrations in Seoul city.

3.3. Potential influences of land-use on the interactions between UHI and air pollutants

Our monitoring stations belonged to two different land-use areas (i.e., residential and industrial areas). We thus hypothesized that the magnitude of UHI and air pollutant concentrations might vary between the two areas. As indicated in Table 8, the mean UHII and air pollutant concentrations were different between residential and industrial areas; UHII and air pollutant concentrations were generally higher in industrial areas than residential areas. For instance, the mean UHII value was 0.32 °C higher in industrial areas than in residential areas. Similarly, mean SO₂, NO₂, CO, O₃, PM10, and PM2.5 Concentrations were, on average, 0.0031 ppm, 0.032 ppm, 0.035 ppm, 0.016 ppm, 1. 361 µg/m³, and 0.005 µg/m³, respectively, higher in industrial areas than residential areas. These mean differences were also statistically significant (p -value < 0.001) for all pollutant concentrations except for PM2.5. To learn more about the potential effect of land-use on the relationship between UHI and air pollution, we conducted Pearson correlations between UHII and air pollutant concentrations and compared correlational strengths between the two land-use categories. As observed in Table 9, UHII is positively correlated with all air pollutant concentrations except for O₃. The observed correlations are also statistically significant. Furthermore, we found that, while the correlational strength between UHI and air

Table 7

Strongest and weakest seasonal effect on the relationship between UHII and air pollutant concentrations.

| | Season | |
|----------------------------|---------------------|---------------------|
| | Strongest (R^2) | Weakest (R^2) |
| CO (ppm) | Autumn (0.346) | Summer (0.00007) |
| NO ₂ (ppm) | Autumn (0.176) | Winter (0.013) |
| O ₃ (ppm) | Autumn (0.512) * | Winter (0.120) |
| PM2.5 (µg/m ³) | Autumn (0.695) * | Winter (0.272) |
| PM10 (µg/m ³) | Winter (0.596) * | Summer (0.122) * |
| SO ₂ (ppm) | Winter (0.849) * | Summer (0.008) * |

Statistically significant results are marked with an asterisk symbol (*). Statistical significance is determined at $P < 0.001$.

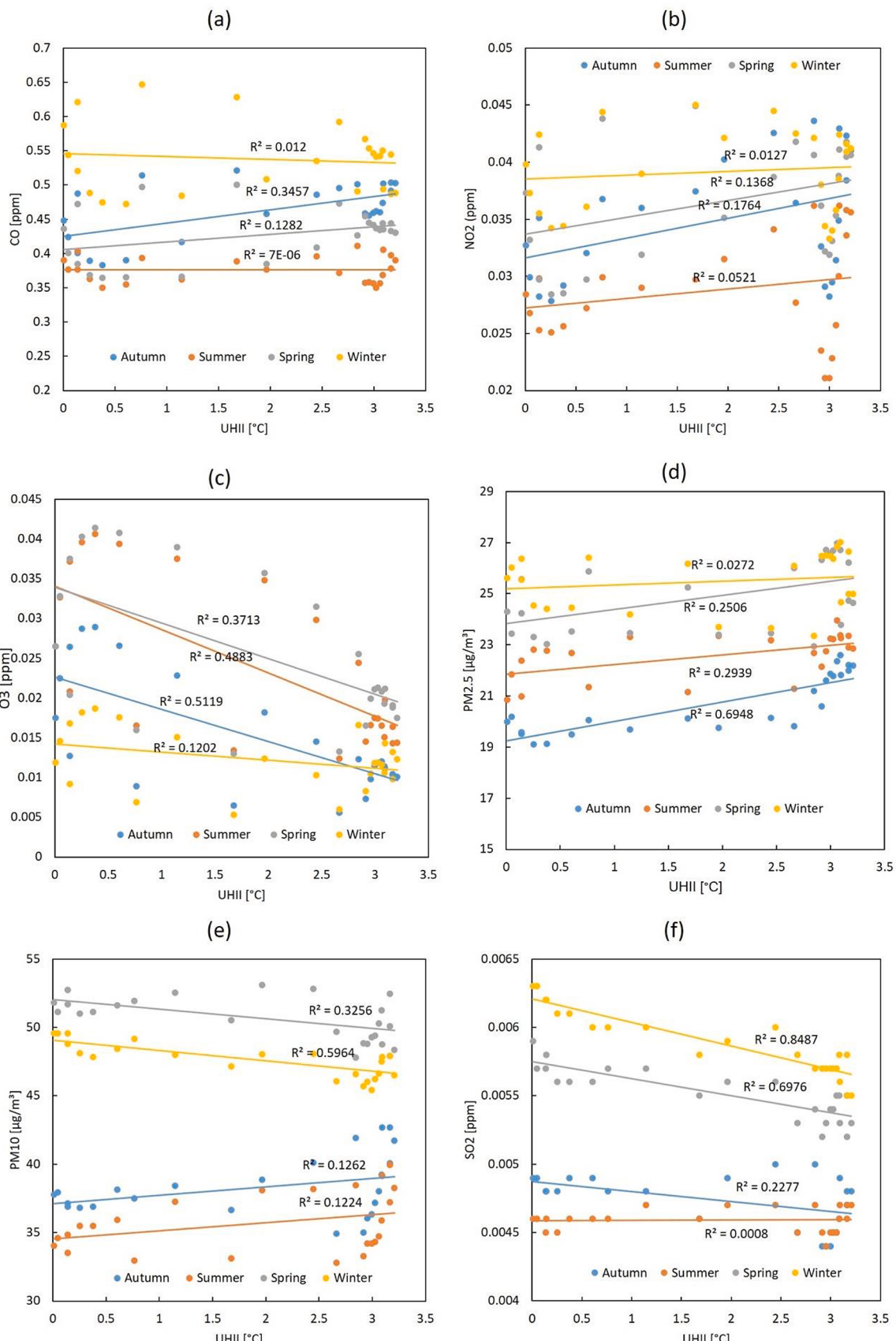


Fig. 5. Seasonal effect on the relationship between UHII and air pollutant concentrations (a) CO (b) NO₂ (c) O₃ (d) PM2.5 (e) PM10 (f) SO₂

Table 8

Mean differences in UHII and air pollutants between industrial and residential stations.

| | Industrial | | Residential | | t-test | |
|------------------------------------|------------|--------|-------------|--------|--------|---------|
| | Mean | SD | Mean | SD | t | p |
| UHII [° C] | 1.84 | 1.731 | 1.52 | 1.76 | 62.11 | < 0.001 |
| SO ₂ [ppm] | 0.0079 | 0.135 | 0.0056 | 0.008 | 6.617 | < 0.001 |
| NO ₂ [ppm] | 0.0653 | 1.200 | 0.0331 | 0.038 | 10.67 | < 0.001 |
| CO [ppm] | 0.5245 | 1.572 | 0.4893 | 1.482 | 7.63 | < 0.001 |
| O ₃ [ppm] | 0.0368 | 0.683 | 0.0209 | 0.191 | 9.39 | < 0.001 |
| PM10 [$\mu\text{g}/\text{m}^3$] | 48.7049 | 38.981 | 47.3442 | 53.531 | 10.46 | < 0.001 |
| PM2.5 [$\mu\text{g}/\text{m}^3$] | 24.7337 | 17.912 | 24.7287 | 18.351 | 0.092 | > 0.001 |

Table 9

Pearson correlations between UHII and air pollutants between industrial and residential stations.

| | Industrial | Residential |
|------------------------------------|------------|-------------|
| SO ₂ [ppm] | 0.017** | 0.004* |
| NO ₂ [ppm] | 0.022** | 0.109** |
| CO [ppm] | 0.042** | 0.027** |
| O ₃ [ppm] | 0.001 | -0.242** |
| PM10 [$\mu\text{g}/\text{m}^3$] | 0.048** | 0.038** |
| PM2.5 [$\mu\text{g}/\text{m}^3$] | 0.094** | 0.098** |

pollutant concentrations varied between the two categories, the variations were not substantial. This finding seems to suggest a consistent UHI effect on the behavior of air pollutants regardless of the land use characteristics. However, it is also worth noting that the number of monitoring stations considered, especially those located in industrial areas, were limited and further studies utilizing data obtained from sparse monitoring stations that include a variety of land-use categories are warranted.

3.4. Potential influences of short-term anthropogenic activities on the relationship between UHI and air pollutants

There are potential differences in UHI and air pollution between weekdays and weekends primarily owing to anthropogenic activities which are likely more pronounced over the weekdays than weekends. We conducted further analysis to learn more about the relationship between UHI and air pollution, considering weekdays and weekends. Weekdays are defined as Monday – Friday, while weekends are defined as Saturday and Sunday. As seen in Table 10, the mean UHII values and air pollutant concentrations were generally higher on weekdays than weekends. These differences were also statistically significant ($p < 0.001$). For instance, it was observed that the mean UHII value during the weekdays was 0.036 °C higher than that during the weekends.

Similarly, the mean SO₂, NO₂, CO, O₃, PM10, and PM2.5 concentrations during the weekdays were approximately 0.00013 ppm, 0.00207 ppm, 0.01559 ppm, 0.00474 ppm, 0.09371 $\mu\text{g}/\text{m}^3$ and 0.20775 $\mu\text{g}/\text{m}^3$ higher than those on weekends. This finding suggests a reduction in both air pollution and UHI during the weekends, possibly due to the low anthropogenic activities prevalent on weekends, especially those

Table 11

Pearson correlations between UHII and air pollutants between weekdays and weekends.

| | Weekdays | Weekends |
|------------------------------------|----------|----------|
| SO ₂ [ppm] | 0.004* | 0.017** |
| NO ₂ [ppm] | 0.109** | 0.022** |
| CO [ppm] | 0.027** | 0.042** |
| O ₃ [ppm] | -0.242** | 0.001 |
| PM10 [$\mu\text{g}/\text{m}^3$] | 0.038** | 0.048** |
| PM2.5 [$\mu\text{g}/\text{m}^3$] | 0.098** | 0.094** |

Statistically significant results are marked with an asterisk symbol (*). Statistical significance is determined at $P < 0.001$.

related to industrial and transportation activities. It is essential to note the mean differences in PM2.5 during the weekdays and weekends were not statistically significant and this is perhaps because its sources (i.e., power generation) are consistent regardless of the day of the week (Gong et al., 2007). Our results regarding increased emissions of air pollutants during the weekdays compared to weekends in Seoul city are reiterated by (Szulejko et al. (2018)). Furthermore, reduced UHII levels during the weekend in Seoul are reported by (Kim and Baik (2005)).

Also, we computed correlations between UHII and air pollutant concentrations separately for weekends and weekdays. As indicated in Table 11, UHII were positively correlated with air pollutant concentrations, except for O₃ which was negatively correlated to UHII, during both the weekdays and weekends. The variation in the strength of the correlation between UHII and air pollution concentrations was relatively the same during both the weekdays and weekends indicating a somewhat consistent interaction between UHII and air pollutant concentrations in Seoul regardless of the day of the week. The negative correlations between UHII and O₃ is likely due to the earlier discussed photochemical reactions (See Eqs. 3–5). However, it is important to highlight that the data used in the current analysis was obtained from a limited number of monitoring stations in Seoul city (see Fig. 1) and future studies employing sparsely-collected datasets are rather warranted to confirm these conclusions. These findings have practical usefulness for policy makers. For example, air pollution regulatory schemes should be stringent during the weekdays when the concentrations of air pollution are likely to be exacerbated by UHI-related temperature increases

4. Conclusions

In the current study, we explore the potential interactions between UHI and air pollution in Seoul city. We found statistically significant interactions between UHI and air pollution concentrations. Generally, most air pollutant concentrations increased with increasing UHI levels; This is mainly because UHI-related warm temperatures modify the thermal structure of urban areas resulting in changes in the dispersion and distribution of air pollutants. We estimated that 1 °C changes in urban temperature could increase SO₂, NO₂, CO, PM10 and PM2.5 by 0.001 ppm, 0.01 ppm, 0.1 ppm, 3 $\mu\text{g}/\text{m}^3$ and 2 $\mu\text{g}/\text{m}^3$, respectively. The relationship between UHI levels and O₃ was negative, although their relationship seems to be influenced by two independent mechanisms rather than from their mere interactions. Furthermore, we found a substantial seasonal effect on the strengths of the relationship between UHII and air pollutant concentrations. The majority of the air pollutants (i.e., CO, NO₂, O₃ and PM2.5) tended to have the strongest relationship with UHII during autumn. However, the relationship between UHII and some of the air pollutants (i.e., PM10 and SO₂) were strongest in winter. The interactions between UHII and air pollutants were nearly nonexistent during the summer period. As such, while there seem to be substantial interactions between UHI and air pollutants, the chemical and physical processes behind such interactions are highly complex and warrant further studies. The results presented in the current manuscript serve as a basis for discussing and exploring such processes in Seoul city.

Table 10

Mean differences in UHII and air pollutants between weekdays and weekends.

| | Weekdays | | Weekends | | t-test | |
|------------------------------------|----------|--------|----------|--------|--------|---------|
| | Mean | SD | Mean | SD | t | p |
| UHII [° C] | 1.65 | 1.755 | 1.61 | 1.767 | 6.61 | < 0.001 |
| SO ₂ [ppm] | 0.0063 | 0.083 | 0.062 | 0.058 | 0.63 | < 0.001 |
| NO ₂ [ppm] | 0.0438 | 0.679 | 0.042 | 0.613 | 1.06 | > 0.001 |
| CO [ppm] | 0.5271 | 0.320 | 0.511 | 0.303 | 16.47 | < 0.001 |
| O ₃ [ppm] | 0.0249 | 0.328 | 0.030 | 0.452 | -3.674 | < 0.001 |
| PM10 [$\mu\text{g}/\text{m}^3$] | 48.2331 | 40.324 | 48.327 | 53.531 | -0.499 | > 0.001 |
| PM2.5 [$\mu\text{g}/\text{m}^3$] | 25.117 | 17.763 | 24.909 | 17.571 | 3.837 | < 0.001 |

5. Limitations and future research

The current research only considers the interactions between air pollutant concentrations and atmospheric UHI derived from in-situ air temperature measurements. However, the dispersion of near-ground air pollutants may behave differently with surface UHI. Future studies, therefore, should attempt to relate air pollution distribution to surface UHI. Such studies would improve our understanding of how UHI mitigative strategies that involve physical transformations of land use (i.e., increased vegetation) could affect air pollution concentrations in urban areas. Also, the current study does not consider the influence of synoptic weather conditions, which may facilitate our understanding of the potential interactions between UHI and air pollution in Seoul, particularly the seasonal interactions discussed in section 3.2. Future studies should attempt to assess the contribution of meteorological variables on the overall interaction between UHI levels and air pollutant concentrations. Another major caveat of the current study is related to the limited number of monitoring stations considered. While the obtained results are meaningful with practical significance for Seoul city, it is still worth noting that Seoul is a large area and the monitoring stations considered represent only a small area. To learn more about the specific interactions between UHI and air pollution, therefore, future studies exploring the said interactions using an extensive network of monitoring stations are warranted. It is also worth noting that the relationship between air pollution and UHI on a city scale (i.e., considering the spatial distribution of UHI and air pollutant concentrations) were not investigated due to the limited number of monitoring stations considered. Nevertheless, the spatial effects, particularly those pertaining to land cover, are likely to have an influence on the behavior of UHI and the likely corresponding behavior of air pollutants need further investigations.

CRediT authorship contribution statement

Jack Ngarambe: Data curation, Formal analysis, Writing - original draft. **Soo Jeong Joen:** Data curation, Formal analysis. **Choong-Hee Han:** Conceptualization, Writing - review & editing. **Geun Young Yun:** Conceptualization, Formal analysis, Writing - original draft, Writing - review & editing, Resources.

Declaration of Competing Interest

None.

Acknowledgement

This work was supported by Korea Institute of Energy Technology Evaluation and Planning (KETEP) grant funded by the Korean government (MOTIE) (20192020101170, Development of Energy-Recovery Ventilators Equipped with Air Filters for Fine Dust Removal).

References

- Akbari, H., Cartalis, C., Kolokotsa, D., Muscio, A., Pisello, A.L., Rossi, F., Santamouris, M., Synnefa, A., Wong, N.H., Zinzi, M., 2016. Local climate change and urban heat island mitigation techniques—the state of the art. *J. Civ. Eng. Manag.* 22 (1), 1–16.
- Anon <http://english.seoul.go.kr/> (accessed on 23/March/2020) <https://doi.org/10.1016/j.enbuild.2019.109402>.
- Arifwidodo, S.D., Tanaka, T., 2015. The characteristics of urban heat island in Bangkok, Thailand. *Procedia - Soc. Behav. Sci.* 195, 423–428. <https://doi.org/10.1016/j.sbspro.2015.06.484>.
- Arnfield, A.J., 2003. Two decades of urban climate research: a review of turbulence, exchanges of energy and water, and the urban heat island. *Int. J. Climatol.* 23, 1–26. <https://doi.org/10.1002/joc.859>.
- Baklanov, A., Lawrence, M., Pandis, S., Mahura, A., Finardi, S., Moussiopoulos, N., Beekmann, M., Laj, P., Gomes, L., Jaffrezo, J.-L., Borbon, A., Coll, I., Gros, V., Sciare, J., Kukkonen, J., Galmarini, S., Giorgi, F., Grimmond, S., Esau, I., Stohl, A., Denby, B., Wagner, T., Butler, T., Baltensperger, U., Buitjes, P., van den Hout, D., van der Gon, H.D., Collins, B., Schluzen, H., Kulmala, M., Zilitinkevich, S., Sokhi, R., Friedrich, R., Theloke, J., Kummer, U., Jalkinen, L., Halenka, T., Wiedensholer, A., Pyle, J., Rossow, W.B., 2010. MEGAPOLI: concept of multi-scale modelling of megacity impact on air quality and climate. *Adv. Sci. Res.* 4, 115–120. <https://doi.org/10.5194/asr-4-115-2010>.
- Basu, R., 2002. Relation between elevated ambient temperature and mortality: a review of the epidemiologic evidence. *Epidemiol. Rev.* 24, 190–202. <https://doi.org/10.1093/epirev/mxf007>.
- Basu, R., 2009. High ambient temperature and mortality: a review of epidemiologic studies from 2001 to 2008. *Environ. Health* 8, 40. <https://doi.org/10.1186/1476-069X-8-40>.
- Borbora, J., Das, A.K., 2014. Summertime urban heat island study for Guwahati City, India. *Sustain. Cities Soc.* 11, 61–66. <https://doi.org/10.1016/j.scs.2013.12.001>.
- Cao, C., Lee, X., Liu, S., Schultz, N., Xiao, W., Zhang, M., Zhao, L., 2016. Urban heat islands in China enhanced by haze pollution. *Nat. Commun.* 7, 12509. <https://doi.org/10.1038/ncomms12509>.
- Choi, Y.-S., Ho, C.-H., Kim, J., Gong, D.-Y., Park, R.J., 2008. The impact of aerosols on the summer rainfall frequency in China. *J. Appl. Meteorol. Climatol.* 47, 1802–1813. <https://doi.org/10.1175/2007JAMC1745.1>.
- Chung, U., Choi, J., Yun, J.I., 2004. Urbanization effect on the observed change in mean monthly temperatures between 1951–1980 and 1971–2000 in Korea. *Clim. Change* 66, 127–136. <https://doi.org/10.1023/B:CLIM.0000043136.58100.ce>.
- Cui, L., Shi, J., 2012. Urbanization and its environmental effects in Shanghai, China. *Urban Clim.* 2, 1–15. <https://doi.org/10.1016/j.uclim.2012.10.008>.
- Dandou, A., Tombrou, M., Schäfer, K., Emeis, S., Protonotariou, A.P., Bossoli, E., Soulakellis, N., Suppan, P., 2009. A Comparison Between Modelled and Measured Mixing-Layer Height Over Munich. *Boundary-Layer Meteorol.* 131, 425–440. <https://doi.org/10.1007/s10546-009-9373-7>.
- Estévez, J., Gavilán, P., Giráldez, J.V., 2011. Guidelines on validation procedures for meteorological data from automatic weather stations. *J. Hydrol. (Amst.)* 402, 144–154. <https://doi.org/10.1016/j.jhydrol.2011.02.031>.
- Fallmann, Joachim., 2014. Numerical Simulations to Assess the Effect of Urban Heat Island Mitigation Strategies on Regional Air Quality. *Diss. Universität zu Köln.*
- Fallmann, J., Forkel, R., Emeis, S., 2016. Secondary effects of urban heat island mitigation measures on air quality. *Atmos. Environ.* 125, 199–211. <https://doi.org/10.1016/j.atmosenv.2015.10.094>.
- Feng, Xiao, Li, Qi, Zhu, Yajie, 2014. Bounding the role of domestic heating in haze pollution of Beijing based on satellite and surface observations. In: 2014 IEEE Geoscience and Remote Sensing Symposium. IEEE, Quebec City, QC, pp. 4772–4775. <https://doi.org/10.1109/IGARSS.2014.6947561>.
- Founda, D., Santamouris, M., 2017. Synergies between Urban Heat Island and Heat Waves in Athens (Greece), during an extremely hot summer (2012). *Sci. Rep.* 7, 10973. <https://doi.org/10.1038/s41198-017-11407-6>.
- Ghanbari Ghozikali, M., Heibati, B., Naddafi, K., Kloog, I., Oliveri Conti, G., Polosa, R., Ferrante, M., 2016. Evaluation of chronic obstructive pulmonary disease (COPD) attributed to atmospheric O₃, NO₂, and SO₂ using air q model (2011–2012 year). *Environ. Res.* 144, 99–105. <https://doi.org/10.1016/j.envres.2015.10.030>.
- Goggins, W.B., Chan, E.Y.Y., Ng, E., Ren, C., Chen, L., 2012. Effect modification of the association between short-term meteorological factors and mortality by urban heat islands in Hong Kong. *PLoS One* 7, e38551. <https://doi.org/10.1371/journal.pone.0038551>.
- Gong, D.-Y., Ho, C.-H., Chen, D., Qian, Y., Choi, Y.-S., Kim, J., 2007. Weekly cycle of aerosol-meteorology interaction over China. *J. Geophys. Res.* 112, D22202. <https://doi.org/10.1029/2007JD008888>.
- Gupta, A., Kumar, R., Kumari, K.M., Srivastava, S.S., 2003. Measurement of NO₂, HNO₃, NH₃ and SO₂ and related particulate matter at a rural site in Rampur, India. *Atmos. Environ.* 37, 4837–4846. <https://doi.org/10.1016/j.atmosenv.2003.07.008>.
- Hamdi, R., Schayes, G., 2008. Sensitivity study of the urban heat island intensity to urban characteristics. *Int. J. Climatol.* 28, 973–982. <https://doi.org/10.1002/joc.1598>.
- Hassid, S., Santamouris, M., Papanikolaou, N., Linardi, A., Klitsikas, N., Georgakis, C., Assimakopoulos, D.N., 2000. The Effect of the Athens Heat Island on Air Conditioning Load, p. 11.
- Iqbal, M.A., Kim, K.-H., Shon, Z.-H., Sohn, J.-R., Jeon, E.-C., Kim, Y.-S., Oh, J.-M., 2014. Comparison of ozone pollution levels at various sites in Seoul, a megacity in Northeast Asia. *Atmos. Res.* 138, 330–345. <https://doi.org/10.1016/j.atmosres.2013.12.003>.
- Jeong, U., Lee, H., Kim, J., Kim, W., Hong, H., Song, C.K., 2013. Determination of the inter-annual and spatial characteristics of the contribution of long-range transport to SO₂ levels in Seoul between 2001 and 2010 based on conditional potential source contribution function (CPSCF). *Atmos. Environ.* 70, 307–317. <https://doi.org/10.1016/j.atmosenv.2013.01.009>.
- Kahl, J.D., 1990. Characteristics of the low-level temperature inversion along the Alaskan Arctic coast. *Int. J. Climatol.* 10 (5), 537–548.
- Khan, Kim, Szulejko, Brown, Jeon, Oh, Shin, Adelodun, 2017. Long-term trends in airborne SO₂ in an air quality monitoring station in Seoul, Korea, from 1987 to 2013. *J. Air Waste Manag. Assoc.* 67, 923–932. <https://doi.org/10.1080/10962247.2017.1305009>.
- Khan, H.S., Paolini, R., Santamouris, M., Caccetta, P., 2020. Exploring the synergies between urban overheating and heatwaves (HWs) in Western Sydney. *Energies*. 13, 470. <https://doi.org/10.3390/en13020470>.
- Khaniabadi, Y.O., Goudarzi, G., Daryanoosh, S.M., Borgini, A., Tittarelli, A., De Marco, A., 2017. Exposure to PM10, NO₂, and O₃ and impacts on human health. *Environ. Sci. Pollut. Res.* 24, 2781–2789. <https://doi.org/10.1007/s11356-016-8038-6>.
- Kim, Y.-H., Baik, J.-J., 2002. Maximum urban heat island intensity in Seoul. *J. Appl. Meteorol.* 41, 9.
- Kim, Y.-H., Baik, J.-J., 2005. Spatial and temporal structure of the urban heat island in Seoul. *J. Appl. Meteorol.* 44, 591–605. <https://doi.org/10.1175/JAM2226.1>.

- Kim, K.-H., Kim, M.-Y., 2003. The effects of Asian Dust on particulate matter fractionation in Seoul, Korea during spring 2001. *Chemosphere*. 51, 707–721. [https://doi.org/10.1016/S0045-6535\(03\)00036-5](https://doi.org/10.1016/S0045-6535(03)00036-5).
- Kim, K.-H., Sul, K.-H., Szulejko, J.E., Chambers, S.D., Feng, X., Lee, M.-H., 2015. Progress in the reduction of carbon monoxide levels in major urban areas in Korea. *Environ. Pollut.* 207, 420–428. <https://doi.org/10.1016/j.envpol.2015.09.008>.
- Klumpp, A., Ansel, W., Klumpp, G., Calatayud, V., Pierre Garrec, J., He, S., Peñuelas, J., Ribas, Á., Ro-Poulsen, H., Rasmussen, S., Sanz, M.J., Vergne, P., 2006. Ozone pollution and ozone biomonitoring in European cities. Part I: ozone concentrations and cumulative exposure indices at urban and suburban sites. *Atmos. Environ.* 40, 7963–7974. <https://doi.org/10.1016/j.atmosenv.2006.07.017>.
- Kolokotroni, M., Giannitsaris, I., Watkins, R., 2006. The effect of the London urban heat island on building summer cooling demand and night ventilation strategies. *Sol. Energy* 80, 383–392. <https://doi.org/10.1016/j.solener.2005.03.010>.
- Kotamarthi, Veerabhadra R., Carmichael, Gregory R., 1990. The long range transport of pollutants in the Pacific Rim region, *Atmospheric Environment. Part A. General Topics* 24 (6), 1521–1534.
- Kouis, P., Kakkoura, M., Ziogas, K., Paschalidou, A.K., Papatheodorou, S.I., 2019. The effect of ambient air temperature on cardiovascular and respiratory mortality in Thessaloniki, Greece. *Sci. Total Environ.* 647, 1351–1358. <https://doi.org/10.1016/j.scitotenv.2018.08.106>.
- Kug, J.-S., Ahn, M.-S., 2013. Impact of urbanization on recent temperature and precipitation trends in the Korean peninsula. *Asia-Pacific J Atmos Sci.* 49, 151–159. <https://doi.org/10.1007/s13143-013-0016-z>.
- Lai, L.-W., Cheng, W.-L., 2009. Air quality influenced by urban heat island coupled with synoptic weather patterns. *Sci. Total Environ.* 407, 2724–2733. <https://doi.org/10.1016/j.scitotenv.2008.12.002>.
- Lee, H.J., Son, Y.-S., 2016. Spatial variability of AERONET aerosol optical properties and satellite data in South Korea during NASA DRAGON-Asia campaign. *Environ. Sci. Technol.* 50, 3954–3964. <https://doi.org/10.1021/acs.est.5b04831>.
- Lee, C.-T., Chuang, M.-T., Chan, C.-C., Cheng, T.-J., Huang, S.-L., 2006. Aerosol characteristics from the Taiwan aerosol supersite in the Asian yellow-dust periods of 2002. *Atmos. Environ.* 40, 3409–3418. <https://doi.org/10.1016/j.atmosenv.2005.11.068>.
- Lee, Y.Y., Kim, J.T., Yun, G.Y., 2016. The neural network predictive model for heat island intensity in Seoul. *Energy Build.* 110, 353–361. <https://doi.org/10.1016/j.enbuild.2015.11.013>.
- Li, D., Bou-Zeid, E., 2013. Synergistic interactions between Urban Heat Islands and heat waves: the impact in cities is larger than the sum of its parts. *J. Appl. Meteor. Climatol.* 52, 2051–2064. <https://doi.org/10.1175/JAMC-D-13-02.1>.
- Li, H., Meier, F., Lee, X., Chakraborty, T., Liu, J., Schaap, M., Sodoudi, S., 2018. Interaction between urban heat island and urban pollution island during summer in Berlin. *Sci. Total Environ.* 636, 818–828. <https://doi.org/10.1016/j.scitotenv.2018.04.254>.
- Lin, W., Xu, X., Ma, Z., Zhao, H., Liu, X., Wang, Y., 2012. Characteristics and recent trends of sulfur dioxide at urban, rural, and background sites in North China: effectiveness of control measures. *J. Environ. Sci.* 24, 34–49. [https://doi.org/10.1016/S1001-0742\(11\)60727-4](https://doi.org/10.1016/S1001-0742(11)60727-4).
- Ling, O.H.L., Ting, K.H., 2010. *Urban Growth and Air Quality in Kuala Lumpur City. Malaysia*, p. 6.
- Liu, W., Ji, C., Zhong, J., Jiang, X., Zheng, Z., 2007. Temporal characteristics of the Beijing urban heat island. *Theor. Appl. Climatol.* 87, 213–221. <https://doi.org/10.1007/s00704-005-0192-6>.
- Loosmore, G.A., Cederwall, R.T., 2004. Precipitation scavenging of atmospheric aerosols for emergency response applications: testing an updated model with new real-time data. *Atmos. Environ.* 38, 993–1003. <https://doi.org/10.1016/j.atmosenv.2003.10.055>.
- Mardia, K.V., 2020. *Measures of Multivariate Skewness and Kurtosis With Applications* (n.d.), p. 12.
- Oh, I.-B., Kim, Y.-K., Hwang, M.-K., Kim, C.-H., Kim, S., Song, S.-K., 2010. Elevated ozone layers over the Seoul Metropolitan Region in Korea: evidence for long-range ozone transport from Eastern China and its contribution to surface concentrations. *J. Appl. Meteor. Climatol.* 49, 203–220. <https://doi.org/10.1175/2009JAMC2213.1>.
- Oh, J.W., Ngarambe, J., Duhirwe, P.N., Yun, G.Y., Santamouris, M., 2020. Using deep-learning to forecast the magnitude and characteristics of urban heat island in Seoul Korea. *Sci. Rep.* 10, 3559. <https://doi.org/10.1038/s41598-020-60632-z>.
- Oke, T.R., 2020. Initial Guidance to Obtain Representative Meteorological Observations at Urban Sites (n.d.), p. 52.
- Oke, T.R., Johnson, G.T., Steyn, D.G., Watson, I.D., 1991. Simulation of surface urban heat islands under 'ideal' conditions at night Part 2: diagnosis of causation. *Boundary. Meteorol.* 56 (4), 339–358.
- Olmo, N.R.S., do, P.H., Saldiva, N., Braga, A.L.F., Lin, C.A., de, U., Santos, P., Pereira, L. A.A., 2011. A review of low-level air pollution and adverse effects on human health: implications for epidemiological studies and public policy. *Clinics*. 66, 681–690. <https://doi.org/10.1590/S1807-59322011000400025>.
- Paravantis, J., Santamouris, M., Cartalis, C., Efthymiou, C., Kontoulis, N., 2017. Mortality associated with high ambient temperatures, heatwaves, and the urban heat island in Athens, Greece. *Sustainability*. 9, 606. <https://doi.org/10.3390/su9040606>.
- Perkauskas, D., Mikeliniskiene, A., 2020. Evaluation of SO₂ and NO_x Concentration Levels in Vilnius (Lithuania) Using Passive Diffusion Samplers (n.d.), p. 4.
- Ray, S., Kim, K.-H., 2014. The pollution status of sulfur dioxide in major urban areas of Korea between 1989 and 2010. *Atmos. Res.* 147–148, 101–110. <https://doi.org/10.1016/j.atmosres.2014.05.011>.
- Runnalls, K.E., Oke, T.R., 2000. Dynamics and controls of the near-surface heat island of Vancouver, British Columbia. *Phys. Geogr.* 21, 283–304. <https://doi.org/10.1080/02723646.2000.10642711>.
- Sarrat, C., Lemonsu, A., Masson, V., Guedalia, D., 2006. Impact of urban heat island on regional atmospheric pollution. *Atmos. Environ.* 40, 1743–1758. <https://doi.org/10.1016/j.atmosenv.2005.11.037>.
- Swamy, G., Nagendra, S.M.S., Schlink, U., 2017. Urban heat island (UHI) influence on secondary pollutant formation in a tropical humid environment. *J. Air Waste Manage. Assoc.* 67, 1080–1091. <https://doi.org/10.1080/10962247.2017.1325417>.
- Szulejko, J., Adelodun, A., Kim, K.-H., Seo, J., Vellingiri, K., Jeon, E.-C., Hong, J., Brown, R., 2018. Short and long-term temporal changes in air quality in a Seoul Urban Area: the Weekday/Sunday effect. *Sustainability*. 10, 1248. <https://doi.org/10.3390/su10041248>.
- Thi Nguyen, H., Kim, K.-H., 2006. Evaluation of SO₂ pollution levels between four different types of air quality monitoring stations. *Atmos. Environ.* 40, 7066–7081. <https://doi.org/10.1016/j.atmosenv.2006.06.011>.
- Yassin, M.F., Al-Shatti, L.A., Al Rashidi, M.S., 2018. Assessment of the atmospheric mixing layer height and its effects on pollutant dispersion. *Environ. Monit. Assess.* 190, 372. <https://doi.org/10.1007/s10661-018-6737-9>.
- Yoshikado, Hiroshi, Tsuchida, Makoto, 1996. High levels of winter air pollution under the influence of the urban heat island along the shore of Tokyo Bay. *J. Appl. Meteorol.* 35 (10), 1804–1813.
- Yun, G.Y., Ngarambe, J., Duhirwe, P.N., Ulpiani, G., Paolini, R., Haddad, S., Vasilakopoulou, K., Santamouris, M., 2020. Predicting the magnitude and the characteristics of the urban heat island in coastal cities in the proximity of desert landforms. The case of Sydney. *Science of The Total Environment*. 709, 136068. <https://doi.org/10.1016/j.scitotenv.2019.136068>.
- Zhao, L., Oppenheimer, M., Zhu, Q., Baldwin, J.W., Ebi, K.L., Bou-Zeid, E., Guan, K., Liu, X., 2018. Interactions between urban heat islands and heat waves. *Environ. Res. Lett.* 13, 034003. <https://doi.org/10.1088/1748-9326/aa9f73>.